Laboratory for Computational Proteomics

www.FenyoLab.org

E-mail: Info@FenyoLab.org

Facebook: *NYUMC Computational Proteomics Laboratory*

Twitter: *@CompProteomics*

Computer experiments on molecular ejection from an amorphous solid: Comparison to an analytic continuum mechanical model

D. Fenyö
Division of Ion Physics, Department of Radiation Sciences, Uppsala University, Box 535, S-751 21 Uppsala, Sweden

R. E. Johnson
Engineering Physics, Thornton Hall, The University of Virginia, Charlottesville, Virginia 22903
(Received 9 March 1992)

Molecular-dynamics simulations are performed to investigate the ejection into the gas phase of large molecules in an amorphous van der Waals solid due to a rapid expansion of a cylindrical "track" of material. Such an excitation geometry may be caused by a fast ion penetrating a solid. The ejection yield, the angular distribution of ejected particles, and the crater size are investigated as a function of the expansion rate and energy, sample thickness, and angle of incidence. Comparisons are made with results from an analytic continuum mechanical model which estimates the ejection from the transiently pressurized region. Although the model is described for point particles and is independent of excitation mechanism, it is able to describe many aspects of the simulation.

INTRODUCTION

The bombardment of the surface of a volatile insulator by heavy MeV particles may result in the ejection into the gas phase of a volume of material.[1,2] Although the details of the conversion of the deposited energy into molecular ejection from the solid surface may be complicated, the excitation densities deposited in a narrow region produce an abruptly formed, high pressure, cylindrical region in the solid, the evolution of which can be followed by continuum mechanics. There are several energy-transfer mechanisms suggested to describe how the excitation and ionization energy deposited by an incident fast ion in an insulator can be converted into atomic and molecular motion.[3] All these mechanisms predict that in the cylindrical "track" the molecules are highly excited having a large amount of energy in internal degrees of freedom, which can include fragmentation. It has also been shown that a fraction of this internal energy can be converted into center of mass motion in a short time (10^{-13}–10^{-12} s).[4,5] This can give rise to a transiently pressurized cylindrical disturbance, which we have referred to as a "pressure pulse." At the vacuum interface the transiently pressurized region can cause ejection of material from the solid.[6]

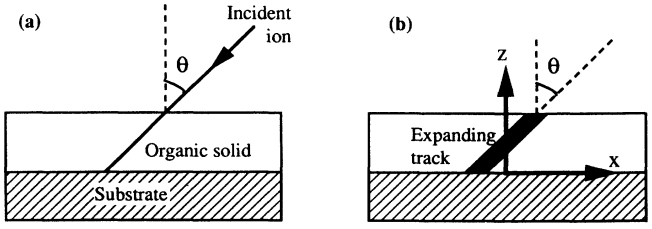

FIG. 1. An MeV ion penetrating an organic solid (a), which will deposit excitation energy around its straight trajectory that will give rise to a local expansion of the material (b).

In the simulations presented here the excited molecules are assumed to transfer energy to the lattice by their physical expansion.[4,5,7,8] The effects of the rapidly expanding molecules in a cylindrical track in an amorphous solid (Fig. 1) are then investigated by molecular-dynamics simulations and compared to aspects of an analytic, continuum mechanical model.[6] This is an extension of earlier work in which the angular distribution of the ejecta and the total yield were calculated and compared.[7–9] Comparisons between results of molecular-dynamics simulations and laboratory experiments on fast heavy-ion-induced ejection of molecules from organic solids have been described earlier,[5,7–11] as have comparisons between experiments and analytic models.[3,4,6,12] Because the molecular-dynamics calculations are in general time consuming, it is extremely useful to confirm the details of analytic models as they can give useful physical insight when explaining experimental data. Further, such models can guide extensions of the physics of desorption to other geometries: desorption by laser pulses[13] and by cluster-ion bombardment.[14] Although comparisons are made here with a model in which the effect produced by the deposited energy is represented by a sum of impulses (pressure-pulse),[6,13] it is very closely related to the "shock-wave"[12,15] and the "gas-flow"[16] models for fast-ion induced sputtering. In each of these models the transient disturbance to the material is treated approximately using a somewhat different starting point (Appendix B).

SIMULATIONS

Details of the simulation procedure and the potentials used are given in an earlier article[8] and the geometry of the model is given in Fig. 1. The simulations were performed for a roughly, cylindrical amorphous solid consisting of, for convenience, spherical particles representing large molecules and interacting via a modified Lennard-Jones pair potential (Appendix A). Newton's

second law for the particles in the solid was made discrete according to the method of Verlet[17] by introducing a time step of 10^{-14} s. This time step was chosen to keep the fluctuations in the total-energy small producing a negligible influence on the results presented. The solid was constructed by placing the particles in each layer independently in close-packed circles. Before simulating the excitation of the solid by an incident ion, the sample was made amorphous by first raising the temperature of the particles then cooling the system to room temperature, taking away 0.01% of the total kinetic energy in each time step until the solid is fully relaxed.

As stated above, the lattice energy of the excited, large molecules was created by simply expanding the molecules by a fraction of their initial radius. This procedure may at first appear artificial. However, the electronically excited track directly produces a net repulsion[18] or the electron energy is distributed among internal modes so that the excited molecules are, on the average, expanded[4] and, therefore, act repulsively.[19] The results obtained from such an expansion have been shown to be very similar to results produced by vibrationally exciting a track of diatomic molecules.[5] In addition, having hard cores is roughly consistent with the large differences in frequencies when the time scales for ejection are very short, as is the case here. For nanosecond laser excitation, on the other hand, the details of the coupling between internal and lattice modes are important.

The effect of the excitation (defined in Appendix A) on a short-time scale was investigated by simulating the classical trajectories of the particles for 200 ps. The expanded molecules cause a change in the potential energy, so that the force between neighbors becomes briefly repulsive and a transiently pressurized region is produced. In response to this pressure pulse both the initially expanded molecules and neighbors, which were not expanded are ejected.[7–9] The magnitude of the pressure pulse can be characterized by the increase in potential energy per unit path length $(dE/dx)_{\text{eff}}$. When comparing to experiments $(dE/dx)_{\text{eff}}$ represents that part of the energy deposited by a fast ion that is converted into track expansion energy. The simulations were mainly performed on a DECstation 5000/200. For the thickest samples, which contained about 20 000 particles, the simulation of one impact took about 50 h.

The finite number of particles makes it necessary to consider the effect of the boundaries on the results of the simulations, e.g., reflection of energy. The cylindrical boundary of the sample $[x^2+y^2=$ (sample radius)$^2]$ is, like the surface, a vacuum interface in our simulations. The effect of this was investigated by changing the sample radius but keeping the sample thickness constant. For the sample dimensions used, the variations of both yield and velocity distributions were within the variations caused by sample inhomogeneity. At the lower surface, (the substrate in an experiment) the boundary condition can affect the yield as is demonstrated in Fig. 2. The thickness dependence of the yield is shown for samples with a reflecting and a free boundary at $z=0$. For thick films, the yield is independent of the boundary condition but for samples that are only a few layers thick the yield is higher for the energy reflecting boundary. Of course, substrates have also been shown to affect the measured yields.[20,21] However, since the ejected ions, rather than neutrals, are the species usually detected (about 0.1% of the ejecta[1]), the relative importance of the role of energy reflection vs the fact that the substrate can supply electrons for neutralization has not been separated.

SIMULATION RESULTS

The rapid rise in potential energy due to the expansion of the particles in the track is converted into kinetic energy in a few picoseconds in this simulation, resulting in steep radial and out-of-the-surface pressure gradients. The resulting pressure pulse, indicated by the changing gradient in the energy density,[6] acts on the particles in the solid. If the *net* force on a particle normal to the surface from the transiently pressurized region is large enough and has a duration long enough to separate it from its neighbors, the surface particle will be ejected. Subsequently, particles below the surface will be ejected. Four examples of the component of the force along the surface normal on particles close to the surface are shown in Fig. 3. Whether the particles are ejected or not is seen to depend not only on the magnitude of the force but also on the local geometry. That is, the applied force must be able to produce a *net outward momentum* large enough to overcome the binding, as seen for (a) and (c) in Fig. 3. The component of the force normal to the surface, for particles that are ejected from the surface layer, can have a few maxima followed by a small negative minimum, i.e.,

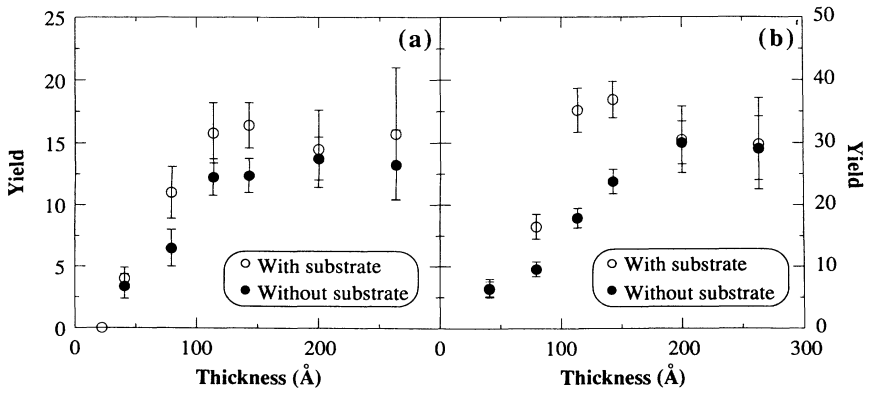

FIG. 2. The yield as a function of the sample thickness for $(dE/dx)_{\text{eff}}$ of (a) 5 eV/Å and (b) 7 eV/Å for two different boundary conditions at $z=0$.

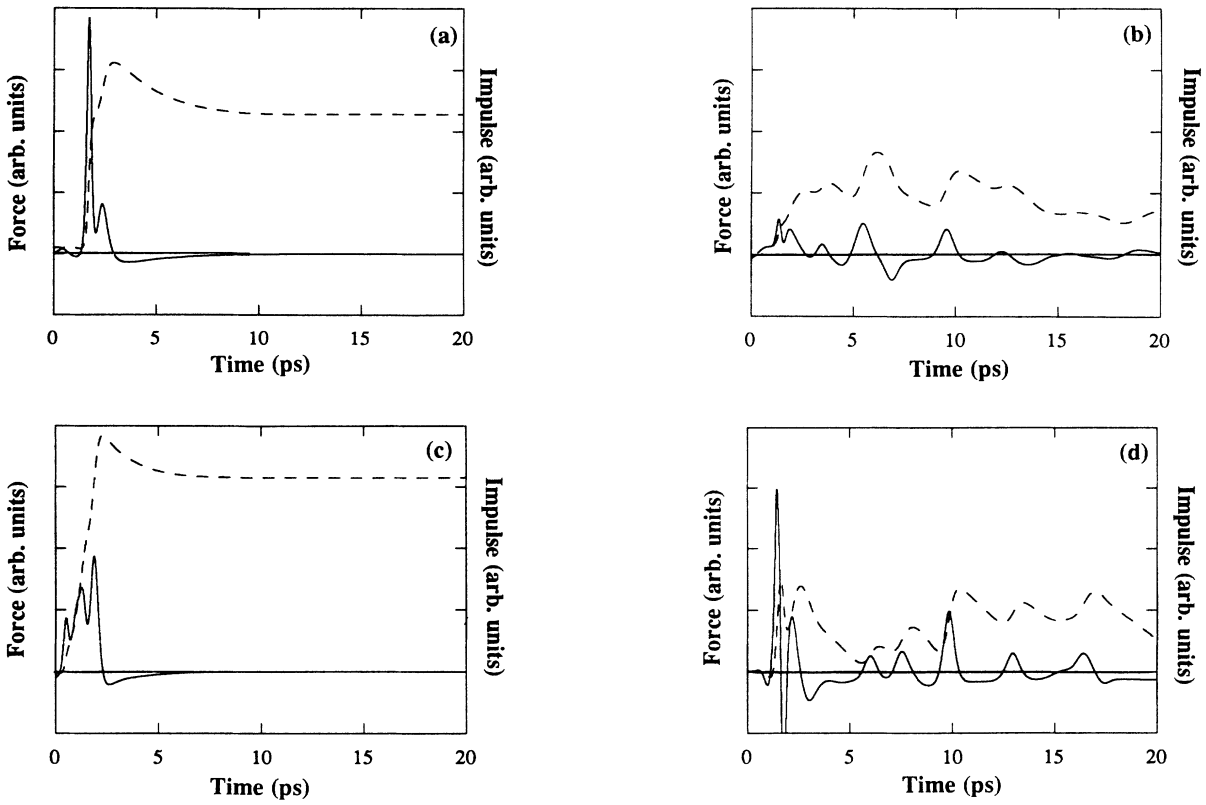

FIG. 3. The z component of the force (solid line) on four different surface molecules as a function of time after expansion giving the accumulated impulse (dashed line). Two of the molecules (a and c) are ejected, and the other two (b and d) are not ejected.

the final attraction to the surface.

Not only are single particles ejected, but also clusters (e.g., dimers, trimers, etc.). At time zero the "internal" potential energy between a pair of neighbors is approximately -0.5 eV, which means that the two particles are close to their equilibrium position in the solid. An increase in both internal and "external" potential energy occurs at the arrival of the pressure pulse. For a while the internal potential energy can be higher than what is required for separation of the two particles, but if energy is transferred to the surrounding particles a dimer can be ejected without decomposing. Approximately 10% of the ejected molecules are dimers in these simulations.

ENERGY TRANSPORT

Energy transport from the abruptly expanded region can occur by shock propagation, by ejection of material from the surface, and by collisional (diffusive) transport. That is, a rapidly moving disturbance is always seen,

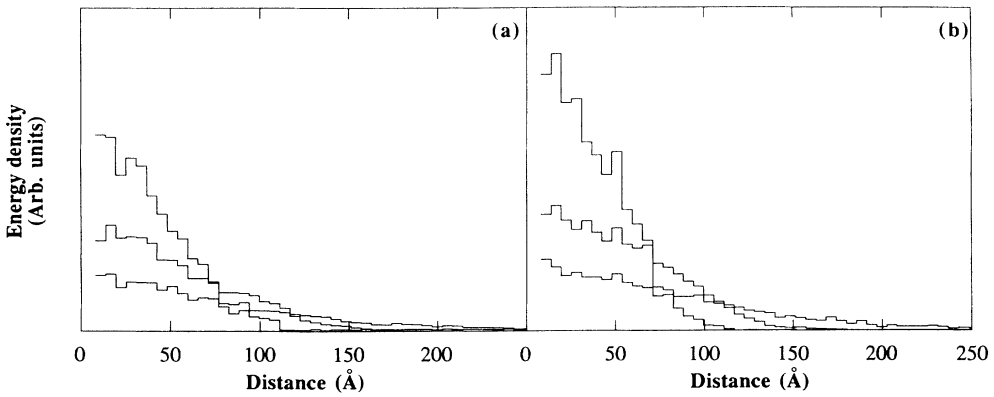

FIG. 4. The energy density profile as a function of time for (a) a 140-Å sample with sputtering and (b) an infinitely thick sample (no sputtering): curves at 0.8, 2, 8 ps.

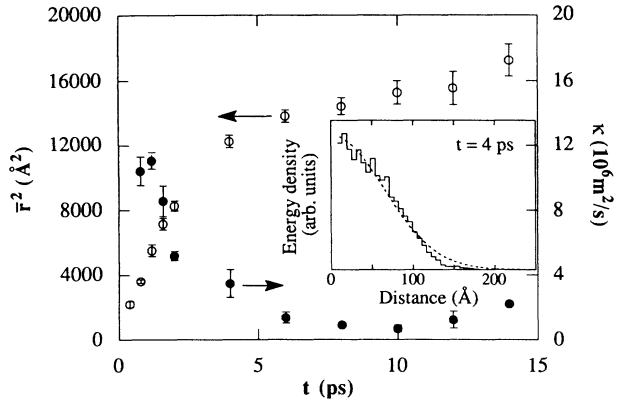

FIG. 5. The radial energy density profile for infinite thickness (no surface) roughly fitting a Gaussian shape, Eq. (B4) (inset): mean-square radius of profile $\bar{r}^2$ and effective diffusivity κ are shown vs time.

which reaches the cylindrical boundary in times of the order of a few times 10^{-12} s. This is the solid-state, acoustic wave signal from the expansion seen also in other simulations.[22] It is a remnant of a weak shock with "back pressure,"[23] which for these excitation densities becomes an acoustic wave beyond the track ($\sim$20 Å) in less than 10^{-12} s. (There may also be an earlier Coulomb repulsive shock extending over distances of the order of a nanometer in times less than 10^{-13} s.[12] This stage is, of course, absent from this model, but would contribute to the total material expansion energy,[3] our starting point.) This is followed by a slower "diffusive" collisional transport of the energy of lattice motion from the transiently pressurized region. In Fig. 4 we compare the radial evolution of this energy between a sample having a vacuum interface at the surface, from which sputtering occurs, and a sample with periodic boundary conditions in the z direction (no sputtering, an essentially infinite sample). Note that for the sample thickness used ($d=140$ Å) and the number of molecules ejected (160) a significant amount of energy is lost to the sputter ejecta.

In a randomly ordered solid it was assumed in Ref. 6 that the collisional, radial energy transport could be approximated diffusively, and a constant diffusivity was used to obtain an analytic solution (Appendix B). That such transport occurs is born out by the radial energy profile in Fig. 4. For times less than 10 ps an average diffusivity of $\kappa \approx 0.05$ cm^2/s roughly describes the calculated radial spread (Fig. 5) (of the order of the speed of sound in our material, 2.6×10^5 cm/s times the molecular size, as for a gas-phase diffusivity). Here we again emphasize an important difference between the model material and a material composed of large molecules. Although, large biomolecules are known to be fairly "rigid," unexcited molecules can, in fact, absorb energy from the expansion. Because of the large numbers of internal degrees of freedom, the heat capacity is large and, therefore, the thermal diffusivity (associated with *local thermodynamic equilibrum) is very small. The relatively large* effective diffusivity in our computer experiments is the rapid, collisional (kinetic energy) component. That is, we are describing a *nonequilibrium* process, in which the ejection is complete in less than 10^{-11} s, well before the lattice energy and the internal modes are in thermal equilibrium. Therefore, it is the size of κ during the rapid energy-transfer processes leading to ejection that matters. The "dissipation" of energy into internal modes can, in principle, be included in the numerical and analytic models,[13] primarily affecting the interpretation of the *amount* of expansion energy associated with a particular yield.

YIELD VS EXPANSION RATE

The yield is defined as the number of particles ejected due to the expansion. In Fig. 6 the dependence of the yield on the rise time and the duration of the expansion is shown. For the range of excitation densities used, a rise time shorter than 10^{-12} s is needed for ejection to occur. That is, by our means of "excitation" longer excitation times produce a pulse too weak to break the bonds to the surface molecules. Of course, adiabatic expansion will result in no pressure pulse forming, as the material gradually adjusts to the increased molecular size. The duration of the expansion needed for maximum ejection yield decreases slightly for increasing excitation energy density over our range. Since a signal traveling at the speed of sound in our material over a molecular diameter ($\sim$16 Å) takes about 6×10^{-13} s, this time scale is understandable. That is, the expansion energy should be put in faster than

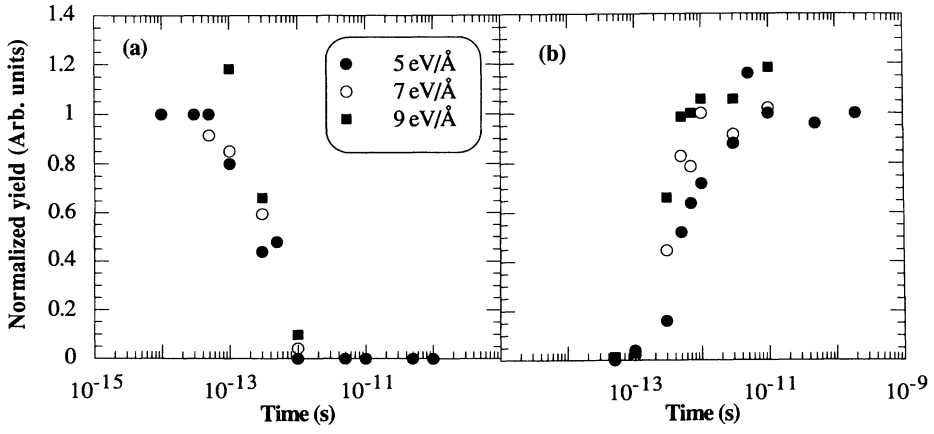

FIG. 6. The normalized yield as a function of (a) the rise time of the expansion (infinite duration) and (b) the duration of the expansion (zero rise time).

the acoustic waves remove it, producing a weak shock.[23,24] For comparison we note that the time it takes for a protein to expand once the breathing mode is excited is about 3×10^{-13} s,[4] and the time for transfer of the vibrational energy to c.m. motion for the highly excited solid of diatomics is about 10^{-12} s.[5,19]

The above results show that the effective pressure pulse is *not* simply dependent on the amount of expansion energy along the cylinder but is also dependent on the rate of excitation, that is on the effective impulse produced. This is also an aspect of the pressure-pulse model.[13] In comparing the simulation with the analytic model we use, in the following, zero rise time and infinite duration. However, when nanosecond lasers excite a material (planar rather than cylindrical geometry) such an assumption is problematic.[13] Here the rapid deposition of energy by the ion followed by the rapid conversion to lattice motion makes such an approximation reasonable.

CONTINUUM MECHANICAL MODEL

The results of the simulation are compared with the results of an approximate, analytic continuum mechanical description.[6,9,13] In that model the sum of the impulses from the transiently pressurized region acting on a volume of material determines the amount of material ejected. To calculate this it is assumed that sources of impulse are created by the incident ion along its track through the solid. The net momentum flux absorbed by a volume can act to eject molecules (i.e., to produce a local phase transform). This is calculated[6] by assuming the energy from the individual sources spreads diffusively in the solid, due to collisional transport, with the net energy density at any time obtained additively. The resulting large energy gradient close to the ion track will produce a volume force on the surrounding material. The *net* impulse transferred to a volume element in the solid is calculated by integrating this force over time, similar to what was shown in Fig. 3 for the molecular-dynamics calculation. A molecule in the solid is regarded as ejected if the z component of this impulse is larger than a critical impulse determined by the cohesive energy of the solid. What is actually calculated in the analytic model is the position in the solid of those molecules that can receive the minimum momentum for ejection. The locus of these positions then determines the volume of ejection. Details are described in Appendix B and Ref. 6, and the relationship to a thermal spike model is discussed in Ref. 6. Note that the resulting expressions parallel those given in Ref. 12, which describes the effect of shock waves (see also Appendix of Ref. 6). The principle differences between these models are the description of the energy transport and the criterion for ejection. For example in Ref. 12 either a critical energy density or a critical energy flux must be achieved for ejection, whereas Ref. 6 uses the net impulse received by a molecular volume due to the transiently pressurized region (Appendix B, Ref. 24).

COMPARISONS

The sample film thickness influences the ejection yield, as discussed earlier, Fig. 2. The yield will first increase with increasing sample thickness due to both the increasing amount of material available and the contributions to the pressure pulse from impulses deeper in the sample. As the film thickness increases the yield eventually becomes independent of sample thickness, because the additional contributions to the pressure pulse by increasing the sample thickness have been diluted before reaching the surface. This concept is valid in both the simulations and the analytic model and the results are compared in Fig. 7. The thickness dependence of the yield is also influenced by the angle of incidence [Fig. 7(b)]. It is seen that for grazing incidence a much sharper saturation is obtained. The thickness associated with saturation varies as $(dE/dx)_{\rm eff}$ *in a manner consistent with the continuum mechanical model.* The yield vs thickness has been measured for organic secondary ions,[20,21] exhibiting a dependence similar to that in Fig. 7. However, the dependence of the saturation thickness on $(dE/dx)_{\rm eff}$ is much slower for 45° angle of incidence but closer for normal incidence.[25] Because these experiments *only detect secondary ions* and were done on an ordered Langmuir-Blodgett film of fatty acids care should be taken with comparisons. The results here are for the total yield from an amorphous solid and compare well with the model in Appendix B. Experiments on total yield are needed.

The dependence of the yield on the deposited energy has earlier been simulated for samples on reflecting substrates.[8] In Fig. 8 the simulated ejection yield from a sample without substrate can be seen as a function of $(dE/dx)_{\rm eff}$ for different sample thicknesses, and it is compared with the predictions of the continuum mechanical

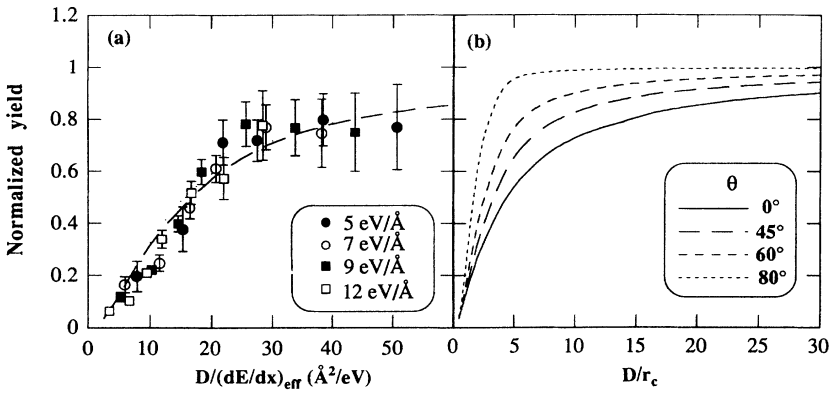

FIG. 7. (a) The normalized yield from a sample without substrate as a function of the thickness (D) divided by $(dE/dx)_{\rm eff}$ for 45° angle of incidence compared with the predictions of the continuum mechanical model (dashed line). (b) The normalized yield obtained from the continuum mechanical model as a function of the thickness divided by the critical radius $r_c \propto (dE/dx)_{\rm eff}$ (see Appendix B) for different angle of incidence.

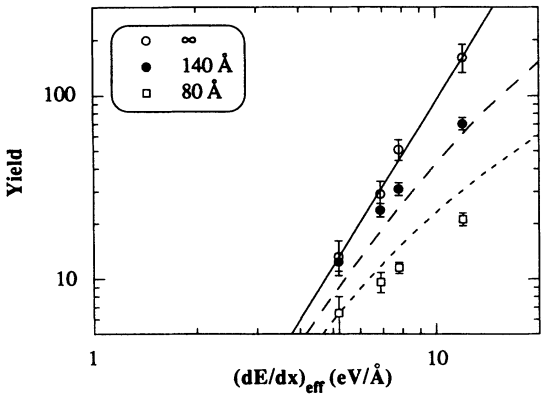

FIG. 8. The yield as a function of $(dE/dx)_{\text{eff}}$ for samples without substrate compared with the predictions of the continuum mechanical model (lines). The infinite thickness means that further increase of the thickness will not affect the yield.

model. The simulated yield from a thick film varies as $(dE/dx)^3_{\text{eff}}$, which is consistent with both experiments on the neutral yield of the amino acid leucine[26] and also with the analytic model for $\beta \approx 0.67$.[8] β, defined in Appendix B, is $(\gamma-1)=(2/3)$ for a *gas* of structureless particles, where γ is the ratio of heat capacities. For thinner films the dependence of the yield on energy deposition in the simulations is *slower* than that in the analytic model.

In Fig. 9 variations of the yield with angle of incidence of the primary particle can be seen for the simulations and the continuum mechanical model. Here we use a technique for calculating the volume ejected like that suggested in Ref. 12 (Appendix B). The increase in yield seen with increasing angle from the normal is due to the larger amount of energy deposited close to the surface and due to the fact that the radial component of the impulse will contribute more favorably. The yield is seen in Fig. 9(b) to have a faster dependence on the angle of incidence for thinner films. Experimentally, the yield of secondary ions from thick organic films has been measured to vary as $\cos^{-n}\theta$, where $n=1-2$.[27] Note, this dependence is also close to that calculated analytically for a cylindrical "thermal" spike model [$\cos\theta^{-1.63}$ (Ref. 28)], emphasizing that the geometry of the excited region is predominantly determining the variation of the yield with incident angle.

CRATER FORMATION

After ejection of some particles, the system will evolve leaving a crater in the sample at the point of "impact" (Fig. 10). A typical pile up of material can be seen at the edges of the crater. Large variations in crater size and shape are obtained due to the statistical nature of the sputtering process consistent with Ref. 22. Indications that a crater is formed in the solid after MeV-ion impact is given by experiments on ordered Langmuir-Blodgett films of fatty acids.[20,21] On an amorphous biomolecular film, we presume the surface layer is the primary source of large-molecule ions, since ejection angles for biomolecule ions are the same when they are adsorbed to a nitrocellulose sample as when they are ejected from a sample of biomolecules.[9] (Note, in Ref. 12 the ion and neutral volumes are assumed to be the same, although in comparison with data on ion ejection angles only surface ejection is included.) There are as yet no measurements on the shape of the volume for the total ejecta for organic solids. However, measurements show that the ion and neutral yields have different (dE/dx) dependencies consistent with their coming from different volumes. This is understandable, since the ionization probability is higher closer to the ion path, where the energy density and the secondary electron flux is also higher, and the neutralization probability is lower for molecules originating from the surface.

The continuum mechanical model of the sputtering process predicts that the volume from which the neutrals originate is roughly hemispherical for normal incidence, with a radius r_c proportional to the electronic stopping power for narrow tracts.[6,29] The result is also obtained in the simulations as seen in Fig. 11. The analytic model does not, of course, describe the thermal rearrangement of the solid seen in Fig. 10. In addition, it is still not known in organic solids if the craters formed in the sputtering process are eventually annealed by the longer-term thermal motion of the surrounding material. However, in mica permanent craters with a radial dependence on the energy loss of the incident close to linear have been observed at high-energy deposition.[30]

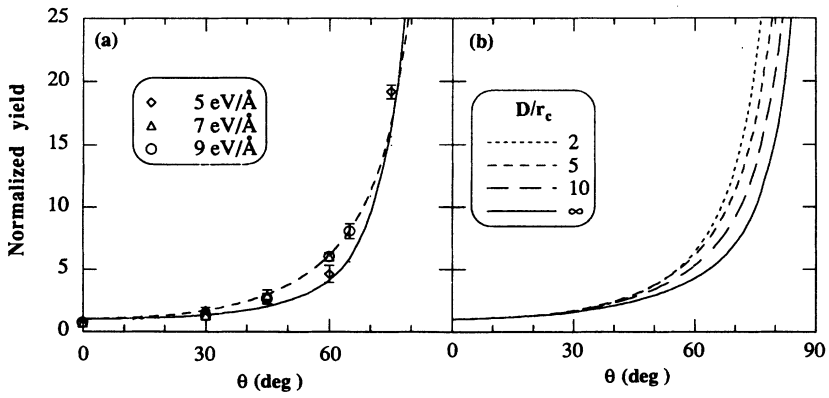

FIG. 9. (a) The yield as a function of the angle of incidence compared with the predictions of the continuum mechanical model (dashed line) and $\cos^{-2}\theta$ (solid line). (b) The normalized yield obtained from the continuum mechanical model as a function of the angle of incidence.

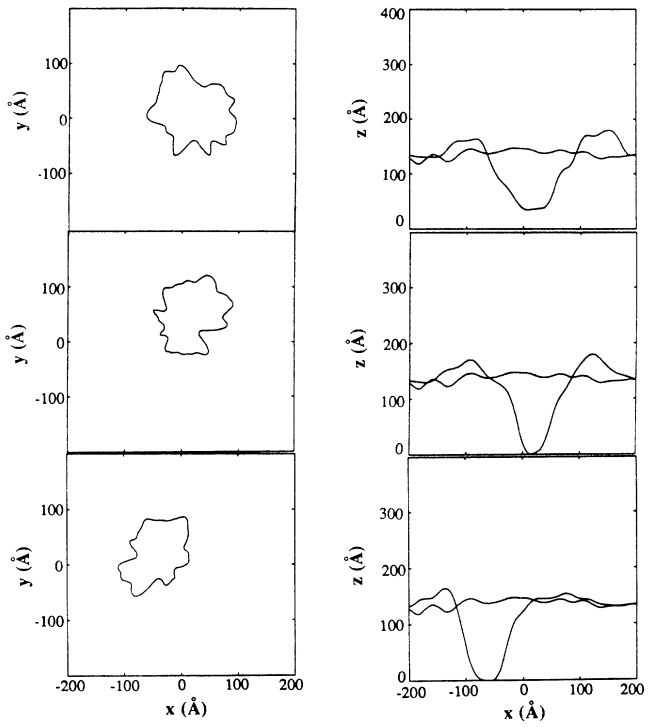

FIG. 10. Smoothed contours of three craters seen from above and from the side, together with the surface before impact, for normal incidence and $(dE/dx)_{\text{eff}}=12$ eV/Å.

CONCLUSIONS

The results of molecular-dynamics simulations, based on a simplified description of the prompt response of the material to a cylindrical excitation, can be used to understand aspects of the ejection of material from an amorphous solid and to reproduce aspects of experimental data on electronic sputtering of large organic molecules. Based on the comparisons made here, along with those discussed earlier,[7–9] it is also seen that many results of these simulations can be described by an approximate analytic model, the so-called pressure-pulse model for sputtering. The concept of the model, based on continuum mechanics, is simple:[6] ejection at the surface is a sum of the effect of the track of impulses from the transiently pressurized region. The analytic expression for point particles in the appendix is obtained by assuming the material acts linearly over the short time periods of interest. For longer time periods the molecular-dynamics simulations indicate that the diffusivity (dispersion of energy) depends on the local energy density. This is the "spike" regime during which additional material may be lost as a result of the random motion of the particles,[6] a sublimationlike process thought to be detrimental to biomolecules.

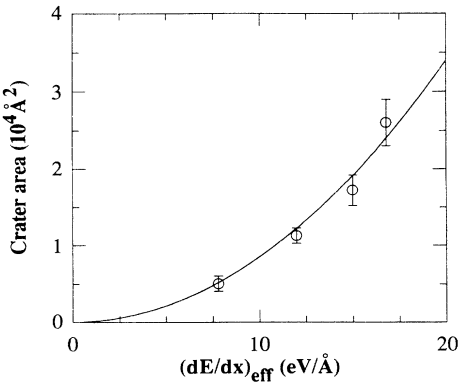

FIG. 11. The area of the crater at the sample surface as a function of $(dE/dx)_{\text{eff}}$ for normal incidence compared with the prediction of the continuum mechanical model (Ref. 6).

As stated earlier, the analytic model used here is closely related to models referred to as shock and gas flow. In the simulation it is seen that the volume must be excited rapidly compared to the rate of acoustic energy transport, so that a weak shock occurs.[23,24] The excited region subsequently expands in response to the pressure gradients in the excited track, producing a transient, hydrodynamic expansion that causes material to leave the solid. Each of the various models attempt to estimate the amount and/or the character of the ejecta using a subset of the properties of the whole process. Although those results, which depend *only on geometry* are essentially the same in these models, the standard shock model calculation of the total yield, as described in Ref. 12, scales as $(dE/dx)_{\text{eff}}^{3/2}$ unlike the simulation results given here, although the authors subsequently modified the ejection criterion (Appendix B). In the calculation of the yield described in Ref. 16 for the gas-flow model, the transient hydrodynamic expansion is approximated by a modified thermal spike, leading to a yield that also differs in its dependence on $(dE/dx)_{\text{eff}}$ from the dependence found in the simulations, but closer to that found in a recent simulation on solid Ar.[31] Although none of the models is a complete continuum mechanical model and although different starting points, can, in principle, lead to the same result, the evolution of the energy and the estimate of the size of the impulse, as calculated in the analytic model described in Appendix B, appears to be quite consistent with the molecular-dynamics simulations made here. Since the analytic model is for point particles the success of this comparison also indicates that the details of the expansion process might *not* be as important as the resulting energy densities achieved.

ACKNOWLEDGMENTS

D. Fenyö would like to acknowledge the Swedish National Science Research Council and the Swedish National board for Technical Development for financial support. R.E. Johnson would like to acknowledge the support of Division of Materials Research and the Astronomy Division of the National Science Foundation and travel grants from the U.S. National Science Foundation and the Swedish National Science Research Council.

APPENDIX A

Parameters for the simulation performed are given below. The numbers inside the brackets are used when explicitly stated. The potential is

$V(d)=E_b[(d_0/d)^{12}-2(d_0/d)^6]$,

$d=|\mathbf{x}_i-\mathbf{x}_j|-2r_c$ (distance between cores),

$r_i=(r_0+\Delta r_i)$ (Δr_i is expansion),

$d_0=r_i+r_j-2r_c$,

$r_0=11$ Å, $r_c=8$ Å, $E_b=0.5$ eV.

The particle mass is

$M=10\,000$ u.

The (cylindrical) sample is

Thickness, $d=140$ Å, (22–410 Å),

Radius=210–410 Å,

Number of molecules=279–20 254,

Density=1.2 gm/cm^3 ,

Bulk Modulus=2.2×10^9 N/m^2.

Boundary conditions are

$z=0$: reflecting substrate,

z=Sample thickness: free boundary,

x^2+y^2=(sample radius)^2: free boundary.

The expansion is

Rise time=0 (10^{-14}–10^{-10} s) ,

Duration=∞ (5×10^{-13}–2×10^{-10} s) ,

$(dE/dx)_{\text{eff}}$=5–17 eV/Å ,

Radius of track=19 Å ,

Angle of incidence, $\theta=45°$ (0–75°) .

APPENDIX B

We first describe the continuum mechanical model based on a sum of impulses including sample thickness dependence and discuss a weak shock at the end. The energy from a point source in the solid (individual molecular expansion) is assumed in Ref. 6 to spread according to

$$\frac{\partial\epsilon(r,t)}{\partial t}=\nabla\cdot[\kappa(\epsilon)\nabla\epsilon(r,t)]-\frac{\epsilon(r,t)}{\tau} , \tag{B1}$$

where ϵ is the energy density, t is the time, τ^{-1} is the energy dissipation rate (e.g., excitation of internal modes, etc.), and κ is the effective diffusivity. This ignores convective transport and the compressibility of the solid, though the latter in an inelastic material can act as a dissipative effect. The spherically symmetric solution of this in an infinite solid for constant κ is

$$\epsilon(r_i,t)=\frac{\Delta E_i}{(\pi\bar{r}^2)^{3/2}}\exp(-r_i^2/\bar{r}^2)\exp(-t/\tau) , \tag{B2}$$

where $\bar{r}^2=r_0^2+4\kappa t$, r_i is the distance from the source, r_0 is the effective radius of the source, and ΔE_i is its energy content. The total-energy density propagation in the solid is obtained by summing the contributions from all sources along the ion trajectory (Fig. 12), i.e., integrating along the z axis from the surface to $D/\cos\theta$,[9] assuming a narrow track,[29]

$$\epsilon(\rho,z,t)=\int_0^{D/\cos\theta}\epsilon(r_i,t)\frac{dz_i}{\lambda_e}$$
$$=\frac{\epsilon(\rho,t)}{2}\left[\text{erf}\left[\frac{D/\cos\theta-z}{r}\right]+\text{erf}\left[\frac{z}{r}\right]\right] , \tag{B3}$$

where

$$\epsilon(\rho,t)=\left[\frac{dE}{dx}\right]_{\text{eff}}\frac{1}{\pi\bar{r}^2}\exp(-\rho^2/\bar{r}^2)\exp(-t/\tau) . \tag{B4}$$

Here D is the sample thickness, θ is the angle of incidence, λ_e^{-1} the number of energy sources per unit path length along the ion trajectory

$$[(\Delta E_i/\lambda_e)=(dE/dx)_{\text{eff}}] .$$

Writing the local pressure as $P\approx\beta\epsilon$, the force on an element of volume in the solid from the momentum equation is given by

$$n_M\mathbf{F}(\rho,z,t)=-\beta\nabla\epsilon(\rho,z,t)=-\frac{d}{dt}(n_M\mathbf{p}) , \tag{B5}$$

where β is a material dependent parameter taken as a constant and n_M the molecular number density. [Note for a gas, $\beta=(\gamma-1)$, where γ is the ratio of specific heats.] The momentum p imparted to an element of volume of the material is obtained by integrating the force in Eq. (B5) over time. For $\tau\rightarrow\infty$ and $r_0\rightarrow0$,

$$\mathbf{p}=p_c r_c\left[-\hat{\mathbf{z}}\left[\frac{1}{r}-\frac{1}{r_1}\right]+\frac{\hat{\boldsymbol{\rho}}}{\rho}\left[\frac{D/\cos\theta-z}{r_1}+\frac{z}{r}\right]\right] , \tag{B6}$$

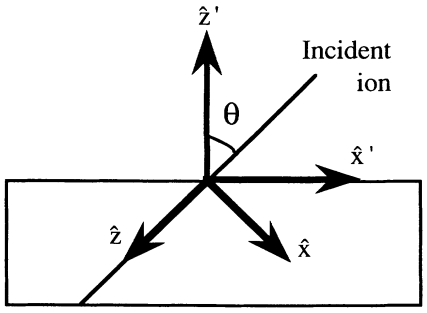

FIG. 12. Definition of coordinates.

where

$$r_c=\beta(dE/dx)_{\text{eff}}/(4\pi\kappa n_M p_c)\propto(dE/dx)_{\text{eff}}/(n_M^{2/3}U)\ ,$$

p_c is the critical impulse for ejection, $r_1=|\mathbf{r}-D\hat{\mathbf{z}}|$, and U is the average cohesive energy. Note that if sharp pulses, rather then diffusive pulses, are used (appendix Ref. 6), Eq. (6) can again be obtained. The components of the momentum[9] from Eq. (B6) are

$$\frac{p_{x'}}{p_c}=\frac{r_c}{r}\left[-\left[1-\frac{r}{r_1}\right]\sin\theta-\frac{x\cos\theta}{\rho^2}\left[r\frac{d/\cos\theta-z}{r_1}+z\right]\right]\ , \tag{B7}$$

$$\frac{p_{y'}}{p_c}=\frac{r_c}{r}\frac{y}{\rho^2}\left[r\frac{D/\cos\theta-z}{r_1}+z\right]\ , \tag{B8}$$

$$\frac{p_{z'}}{p_c}=\frac{r_c}{r}\left[\left[1-\frac{r}{r_1}\right]\cos\theta-\frac{x\sin\theta}{\rho^2}\left[r\frac{D/\cos\theta-z}{r_1}+z\right]\right]\ . \tag{B9}$$

The ejection of a volume of the solid is assumed to be determined by $p_{z'}>p_c$, *if its velocity aims at a part of the* surface above it that is also ejected. This means that a part of the solid will be ejected if it receives a large enough impulse to overcome the cohesive energy of the solid *and that it will not collide with* a part of the solid above it that is *not* ejected. These expressions are easily modified[13] if the pulses are dissipative (τ finite), the time for accumulation of momentum is not infinite, or the track has a finite width.[29] The results presented will be the same as long as r_c is much smaller than the effective transport distance [e.g., $(\kappa\tau)^{1/2}$ when τ finite in Eq. (B1)].

A particularly useful aspect of the model above is the ability to represent the geometry of the excitation additively. Hence, in the appendix of Ref. 6 the above was also obtained for δ-function impulses. Additivity requires linearity of the effect with source function. In a gas strong shocks ($\Delta P\gg P_0$, where ΔP is the pressure excursion in an impulse and P_0 is the ambient pressure) are *not* additive. However, a weak shock $\Delta P\ll P_0$ is, since in one dimension

$$\Delta(n_M\mathbf{p})\approx\Delta P/c\ , \tag{B10}$$

where $\mathbf{p}$ is the momentum applied, as in Eq. (B6), and c is the speed of sound.[23,32] The bulk modulus of the material provides an effective back pressure in the solid and the criterion for a weak shock is density rather than pressure.[23]

In Ref. 12 the pressure excursion in the shock (pulse) divided by the speed of sound is like our $(n_M\mathbf{p})$ in Eq. (B10). However, those authors initially use the local energy density as the ejection criterion, as was the case in Ref. 15. In their more recent paper they stated that the energy density could be used for ion ejection and the energy flux for total yield. In the gas-flow model a temperature (pressure) profile is assumed to have been produced by the incident ion. This profile is then used to calculate the gas flow out of the energized region. For convenience the authors in Ref. 16 use a thermal spike with $U=0$ to calculate the loss of material until the temperature drops below the critical temperature, which is proportional to U. Aspects of this have recently been verified by molecular dynamics.[31]

[1]M. Salehpour, P. Håkansson, B. U. R. Sundqvist, and S. Widdiyasekera, Nucl. Instrum. Methods B **13**, 278 (1986).

[2]B. U. R. Sundqvist, in *Sputtering by Particle Bombardment III,* edited by R. Behrisch and K. Wittmaack (Springer-Verlag, Berlin, 1991).

[3]R. E. Johnson, Int. J. Mass Spectrosc. Ion Proc. **78**, 357 (1987).

[4]P. Williams and B. U. R. Sundqvist, Phys. Rev. Lett. **58**, 1031 (1987).

[5]S. Cui and R. E. Johnson, Int. J. Quantum Chem. 23, 575 (1989); Int. J. Quantum Chem. (to be published); S. Banerjee, R. E. Johnson, P. T. Cummings, and S. T. Cui, Phys. Rev. B **43**, 12 707 (1991).

[6]R. E. Johnson, B. U. R. Sundqvist, A. Hedin, and D. Fenyö, Phys. Rev. B **40**, 49 (1989).

[7]D. Fenyö, B. U. R. Sundqvist, B. R. Karlsson, and R. E. Johnson, J. Phys. (Paris) Colloq. **50**, C2-33 (1989).

[8]D. Fenyö, B. U. R. Sundqvist, B. R. Karlsson, and R. E. Johnson, Phys. Rev. B **42**, 1895 (1990); D. Fenyö, A. Hedin, P. Håkansson, R. E. Johnson, and B. U. R. Sundqvist, in *Ion Formation from Organic Solids (IFOS V),* edited by A. Hedin, B. U. R. Sundqvist, and A. Benninghoven (Wiley, Chichester, 1990), p. 33.

[9]D. Fenyö, Ph.D. thesis, University of Uppsala, 1991.

[10]E. R. Hilf, H. F. Kammer, and B. Nitzschmann, *Ion Formation from Organic Solids (IFOS IV),* edited by A. Benninghoven (Wiley, Chichester, 1989).

[11]E. R. Hilf and H. F. Kammer, J. Phys. (Paris) Colloq. **50**, C2-245 (1989); *Ion Formation from Organic Solids (IFOS V)* (Ref. 8).

[12]I. S. Bitensky, A. M. Goldenberg, E. S. Parilis, in *Ion Formation from Organic Solids V (IFOS V),* edited by A. Hedin, B. U. R. Sundqvist, and A. Benninghoven (Wiley, Chichester,

1990), p. 205; I. S. Bitensky and E. S. Parilis, Nucl. Instrum. Methods **B21**, 26 (1987).

[13]R. E. Johnson, in *Ion Formation from Organic Solids (IFOS V)* (Ref. 8), p. 189; R. E. Johnson, S. Banerjee, B. U. R. Sundqvist, D. Fenyö, and A. Hedin, in *Methods and Mechanics for Producing Ions from Large Molecules* (NATO Science Series), edited by K. Standing and W. Ens (Plenum, New York, 1991), p. 89; R. E. Johnson and B. U. R. Sundqvist, Rapid Commun. Mass Spectrosc. **5**, 574 (1991).

[14]J. F. Mahoney, J. Perel, S. A. Ruatta, P. A. Martino, S. Husain, and T. D. Lee, Rapid Commun. Mass Specosc. **5**, 441 (1991).

[15]Y. Yamamura, Nucl. Instrum. Methods **194**, 515 (1982); G. Carter, *ibid.* **209/210**, 1 (1983).

[16]H. Urbassek and J. Michl, Nucl. Instrum Methods B **22**, 480 (1987); D. E. Darret, T. F. Magnera, R. Tian, and J. Michl, Radiat. Eff. **99**, 247 (1986).

[17]L. Verlet, Phys. Rev. **159**, 98 (1967).

[18]C. C. Watson and T. A. Tombrello, Radiat. Eff. **89**, 263 (1985).

[19]B. Fain and S. H. Lin, J. Chem. Phys. **91**, 2726 (1989).

[20]G. Säve, P. Håkansson, B. U. R. Sundqvist, and U. Jönsson, Nucl. Instrum. Methods B **26**, 571 (1987); G. Säve, P. Håkansson, B. U. R. Sundqvist, E. Söderström, S. E. Lindqvist, and J. Berg, Inst. J. Mass Spectrum. Ion Phys. **78**, 259 (1987); Appl. Phys. Lett. **51**, 1379 (1987).

[21]G. Bolbach, S. Della-Negra, C. Deprun, Y. LeBeyec, and K. G. Standing, Rapid Commun. Mass Spectrom. **1**, 22 (1987).

[22]H. M. Urbassek and K. T. Waldeer, Phys. Rev. Lett. **67**, 105 (1991); K. T. Walder and H. M. Urbassek (unpublished); R. P. Webb and D. E. Harison, Appl. Phys. Lett. **39**, 311 (1981).

[23]Ya. B. Zel'dovich and Yu. P. Raizer, in *Physics of Shock Waves and High-Temperature Hydrodynamic Phenomena,* (edited by W. D. Hayes and R. F. Probstein (Academic, New York, 1967).

[24]R. E. Johnson (unpublished).

[25]R. Schmidt, Ch. Schoppmann, D. Brandl, A. Ostrowski, H. Voit, D. Johannsman, and W. Knoll, Phys. Rev. B **44**, 560 (1991).

[26]A. Hedin, P. Håkansson, M. Salehpour, and B. U. R. Sundqvist, Phys. Rev. B **35**, 7377 (1987).

[27]P. Håkansson, I. Kamensky, and B. Sundqvist, Surf. Sci. **116**, 302 (1982).

[28]R. E. Johnson, J. Phys. (Paris) Colloq. **50**, C2-251 (1989).

[29]D. Fenyö (unpublished).

[30]F. Thibaudau, J. Cousty, E. Balanzat, and S. Bouffard, Phys. Rev. Lett. **67**, 1582 (1991).

[31]H. M. Urbassek, H. Kafemann and R. E. Johnson (unpublished).

[32]L. D. Landau and E. M. Lifshitz, *Fluid Mechanics* (Pergamon, Elmsford, NY, 1987).